Current Science International
Volume: 14 | Issue: 04| Oct. – Dec.| 2025

EISSN:2706-7920 ISSN: 2077-4435
DOI: 10.36632/csi/2025.14.4.16
Journal homepage: www.curresweb.com
Pages: 204-223

Mineralogy, Geochemistry and Radioactivity of Stream Sediments of Wadi Abu Harba-North Eastern Desert, Egypt

Osama M. Draz

Nuclear Materials Authority, Cairo, Egypt, P.O. Box 530, El-Maadi

Received: 15 August 2025 **Accepted:** 10 Oct. 2025 **Published:** 30 Oct. 2025

ABSTRACT

Wadi Abu Harba is located in North Eastern desert. This wadi is surrounded by syenogrenites and alkali feldspar granite with some dyke swarms of acidic and basic composition. The heavy minerals represented by 1.098 % magnetite, 0.3136 % ilmenite, 0.1208 % leucoxene, 0.3732 % rutile, 0.2516 % zircon, 0.01684 % monazite, 0.118 % garnet and 0.1596 % titanite. Radiometric analysis revealed that the average equivalent uranium content (eU) is 1.64 ppm and the average equivalent thorium is (eTh) is 9.64 ppm. On the other hand, the analysis and identification of several separated mineral grains of some stream sediments samples using a scanning electron microscope and X-ray diffraction revealed the presence of several economic minerals. These minerals include zircon, uranothorite, thorianite, monazite, cerite, apatite, fluorite, garnet and hematite. The present study proved that zircon, uranothorite, thorianite and monazite are the main radioactive minerals responsible for the radioactivity of the studied stream sediments and may control the geochemical enrichment of elements such as Th, U, Zr, Y, and Nb.

Keywords: Wadi Abu Harba, North Eastern desert, syenogrenites, alkali feldspar granite, heavy minerals device, Radiometric analysis.

Introduction

The area is located in the North Eastern Desert of Egypt between Longitudes 33^0 $35^/$ $24^{//}$E and 33^0 $45^/$ E and Latitudes 26^0 $45^/$ $43^{//}$ N and 26^0 $50^/$ $36^{//}$ N (Fig. 1). The area under investigation is studied by different authors e.g. Sabet *et al*., (1972) and Akaad *et al*., (1973). The studied granite is one of the most promising uranium occurrences in the North Eastern Desert of Egypt because of its contents of abnormal high level of radioactivity.

The study area covers about 200 km^2, (Fig. 1). It is characterized by rugged topography with moderate to high relief and very arid climate. The present work is concerned with geology of rock unites covering Wadi Abu Harba area, as well as heavy mineral concentrations and radioactivity in stream sediments covering the main wadies dissected the area.

The basement rocks of Wadi Harba area are of Precambrian age and dissected by dry wadi that filled by a wide variety of stream sediments (wadi deposits). These wadies deposits are composed of sands, gravels, and boulders. They are mainly derived from granites containing some variable heavy minerals.

Geologic Setting

Wadi Abu Harba is surrounded by syenogrenites and alkali feldspar granite with some dyke swarms of acidic and basic composition. Syenogranite is cut by sets of faults in addition to the observed network of micro-fissures and joints which play a role of pathways to fluid flows. Abu Harba granites are mainly composed of syenogranite, which have alkaline suite which still preserve their original texture in spite of the effects of hydrothermal alterations. Abd El Atty, (2013) revealed

Corresponding Author: Osama M. Draz, Nuclear Materials Authority, Cairo, Egypt, P.O. Box 530, El-Maadi.

that the syenogranite of Abu Harba and Al Shagola have the chemical characteristics of calc-alkalic to alkalic calcic and metaluminous to slightly peraluminous rocks. It was generated and emplaced in post orogenic environment and described as highly fractionated I-type granites.

Syenogranite rocks in the studied area are coarsegrained and porphyritic with pink to red colors but turn to brownish red when stained with hematite along joints and fractures and speckled with many xenoliths. Syenogranite rocks are cut by one or more sets of faults mostly directed to the NE-SW. The contact between syenogranite and the alkali feldspar granite type especially at the western parts is gradational. On the other hand, this granite intrudes the Dokhan volcanics at its eastern and southern boundaries with irregular contacts. Abu Harba granites altered in some sheared parts due to hydrothermal processes, especially along the fault planes and contacts. Syenogranite is intensely crossed by dyke swarms which are mainly of basic composition. These dykes occur as long ribbons and ridges responsible for the many long narrow parallel ridges seen in the area. They are mostly following the NE-SW and ENE-WSW directions (Abd El Atty, 2013).

Sampling and Methodology

25 stream sediment samples were collected from Wadi Abu Harba (Fig. 2 b & c). Samples are taken by digging a rectangular hole to a depth of 0.7 m (Fig. 2 a). They are investigated mineralogically, chemically for trace elements and radiometrically. Trace elements were analyzed by using X-ray fluorescence (Phillips PW 1410. Radiometrically analysis has been achieved using gamma-ray spectrometry with multi-channel analyzer" to determine uranium (eU) and thorium (eTh). The samples were properly sieved by 1mm before subjecting the liberated size fractions to heavy-mineral separation using bromoform (specific gravity = 2.85 gm/cm3). From the obtained heavy fractions, pure mineral grains were manually picked and investigated under a binocular stereomicroscope. Some of the picked mineral grains were subjected to environmental scanning electron microscope ESEM). This instrument includes a Philips XL 30 energy-dispersive spectrometer (EDS) unit. The applied analytical conditions were an accelerating voltage of 30 KV with a beam diameter of 1-2 µm for a counting time of 60-120 s and a minimum detectable weight concentration ranging from 0.1 wt % to 1 wt %. All these analyses were carried out at the laboratories of the Egyptian Nuclear Materials Authority (NMA).

Fig.1 a): Location map of the study area

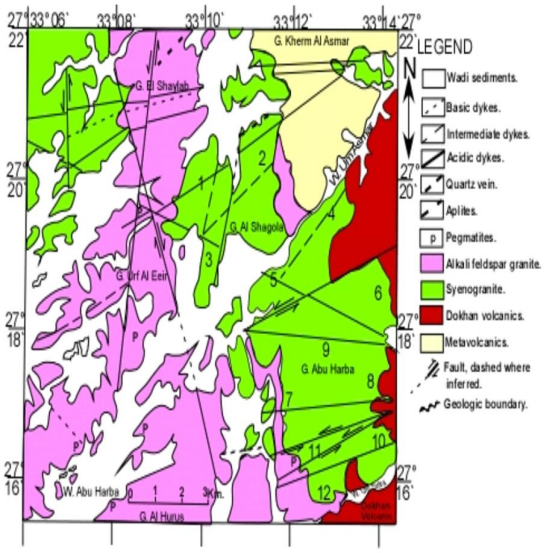

Fig. b): Geological map of the study area (after Abd El Atty, 2013)

Mineralogical Studies

For studying the heavy fractions of the stream sediments samples which collected from Wadi Abu Harba, samples were quartered and sieved which later separated by bromoform. Separated minerals were picked under binocular microscope and identified using ESEM supported by EDX. The

identification of these minerals is confirmed by XRD analysis when enough amounts of separated mineral grains were available. The average content of the heavy minerals in the studied stream sediments is 5.96 % ranging from 1.45 % and 10.45 % (Table 1). The content of heavy minerals in the studied stream sediments increase from north (upstream) to south (downstream).

Fig. 2:
a) Open Pit Drainage pattern
b) Dendritic patterns of Wadi Abu Harba
c) Distribution of collected samples of Wadi Abu Harba

Table 1: Percentages of heavy minerals in the studied stream sediments of Wadi Abu Harba

Sample No.	Heavy Minerals %	Sample No.	Heavy Minerals %
1	2.31	14	5.36
2	3.14	15	7.34
3	1.45	16	5.14
4	4.25	17	6.38
5	4.03	18	8.22
6	3.69	19	7.08
7	4.68	20	6.87
8	5.06	21	8.45
9	4.65	22	8.97
10	5.17	23	9.07
11	5.38	24	10.45
12	6.02	25	9.53
13	6.54		
Min.	1.45 %	Max.	10.45 %
Av.		5.96 %	

Heavy Minerals Distribution

A hand magnet and free-magnetite samples were subjected to the magnetic separation at 0.2, 0.5, 1.0 and 1.5 current amperes. The obtained fractions were weighed and their percentages were calculated (Table 2). It is obviously noted that the heavy minerals are concentrated mainly in 0.2 amp. and 0.5 amp. magnetic fractions, while 1.5 amp magnetic fractions contains the lowest concentration of the heavy minerals.

Table 2: Frequency of heavy minerals in the different magnetic fractions

S. N.	Magnetite %	0.2 mag. %	0.5 mag. %	1.0 mag. %	1.5 mag. %
1	16.63	30.50	44.68	4.12	1.84
2	30.46	25.48	38.73	1.74	0.44
3	17.78	47.65	29.64	2.64	0.61
4	26.79	40.37	12.62	3.69	2.51
5	18.18	37.24	38.43	2.86	1.35
6	28.19	40.13	30.35	1.84	2.05
7	20.18	38.50	38.43	2.65	2.17
8	25.34	35.65	36.65	1.47	1.22
9	18.07	22.46	40.37	3.55	4.22
10	23.18	31.99	45.51	0.87	0.33
11	21.75	46.45	19.44	2.14	0.88
12	26.79	40.34	12.61	3.69	2.51
13	18.17	37.27	38.46	2.88	1.35
14	20.18	38.50	38.45	2.65	2.17
15	17.75	47.64	29.62	2.63	0.61
16	26.79	40.34	12.61	3.67	2.51
17	16.65	30.51	44.69	4.11	1.84
18	16.63	30.51	44.66	4.13	1.84
19	30.46	25.47	38.72	1.72	0.44
20	17.77	47.64	29.62	2.63	0.61
21	30.45	25.46	38.72	1.74	0.44
22	21.78	46.43	19.44	2.12	0.88
23	18.07	22.46	40.38	3.52	4.22
24	23.18	31.98	45.51	0.87	0.33
25	21.75	46.41	19.45	2.14	0.88

Each fraction obtained from the magnetic separation process was microscopically investigated to calculate the frequency distribution of the concerned minerals in the studied stream sediment. A considerable number of grains from each magnetic fraction were counted (about 1500 grains). The weight percentage of each concerned mineral relative to the corresponding original sample was calculated ac- cording to Stakhove equation (1957):

$$Q = [P.\ n.d / \Sigma (nd)].100$$

Where: **Q** = the weight percentages of the concerned mineral
P = the weight percentage of the corresponding magnetic fraction.
n = the number of grains of the mineral.
d = specific gravity of the mineral.
Σ(nd) = the sum. of the number of grains for each mineral multiplied by its specific gravity.

The identified heavy mineral assemblages studied under a Binocular Stereomicroscope can be classified into two main groups according to Folk (1980). The first one is opaque minerals as; magnetite, ilmenite, and leucoxene. The second group is non-opaque minerals includes garnet, rutile, titanite, zircon, monazite, thorite, and green silicates (pyroxene and amphibole groups, epidote, mica group, ect.). The accessory mineral assemblage is responsible for the radioactivity on the studied stream sediments. Consequently, a conspicuous variety of the uraniferous accessory minerals as well as primary thorium minerals have been established. Essentially, the XRD should have taken place on the common minerals, while ESEM is used as a complementary technique for characterizing the rarity ones (Fig. 3). The percentage of each mineral is calculated to the original samples and averages of the total heavy mineral for the studied sediments are tabulated in Table 3.

Table 3: Weight percentages of the concerned heavy opaque minerals in the studied samples.

S. N.	Mag. %	Ilm. %	Leu. %	Ga. %	Rut. %	Tit. %	Zr. %	Mz. %	Th. %	G. S. %
1	1.3	0.5	0.2	0.1	0.3	0.2	0.1	0.04	0.02	2.03
2	1.8	0.8	0.2	0.3	0.5	0.1	0.3	0.07	0.02	3.10
3	1.3	0.6	0.1	0.2	0.6	0.3	0.5	0.03	0.01	1.96
4	2	0.9	0.3	0.4	0.8	0.4	0.6	0.06	0.02	1.50
5	1.2	0.4	0.2	0.2	0.5	0.3	0.4	0.01	0.01	3.69
6	1.3	0.2	0.2	0.3	0.7	0.2	0.5	0.02	0.01	3.78
7	1.3	0.3	0.2	0.1	0.9	0.3	0.7	0.02	0.03	2.55
8	2	0.9	0.3	0.3	1.1	0.5	0.7	0.07	0.01	3.63
9	1.5	0.2	0.1	0.06	0.3	0.4	0.1	0.01	0.01	2.32
10	1.1	0.3	0.1	0.1	0.2	0.3	0.2	0.01	0.02	1.9
11	1.5	0.1	0.3	0.3	0.4	0.2	0.5	0.04	0.02	1.71
12	1.7	0.4	0.3	0.1	0.2	0.1	0.4	0.001	0.02	2.2
13	1	0.6	0.3	0.3	0.3	0.22	0.4	0.001	0.01	3.1
14	2.0	0.2	0.1	0.04	0.25	0.2	0.2	0.01	0.02	3.1
15	1	0.1	0.03	0.03	0.4	0.1	0.1	0.001	0.01	2.9
16	0.8	0.1	0.02	0.01	0.3	0.02	0.08	0.001	0.01	2.7
17	0.9	0.2	0.01	0.02	0.22	0.03	0.08	0.001	0.01	2.5
18	0.8	0.14	0.04	0.02	0.18	0.01	0.05	0.001	0.02	2.8
19	0.7	0.12	0.03	0.02	0.15	0.01	0.05	0.001	0.01	1.6
20	0.6	0.2	0.01	0.01	0.12	0.01	0.04	0.001	0.02	1.4
21	0.9	0.1	0.02	0.01	0.1	0.01	0.03	0.001	0.02	2.2
22	0.4	0.15	0.03	0.03	0.2	0.01	0.02	0.001	0.01	2.2
23	0.4	0.2	0.01	0.04	0.22	0.02	0.05	0.001	0.03	3.1
24	0.15	0.4	0.03	0.04	0.3	0.03	0.07	0.04	0.02	3.2
25	0.1	0.13	0.01	0.03	0.3	0.02	0.02	0.01	0.02	3.3
Min.	0.1	0.1	0.01	0.01	0.1	0.01	0.02	0.001	0.01	1.4
Max.	2.1	0.9	0.4	0.4	1.1	0.5	0.8	0.07	0.03	3.78
Aver.	1.097	0.3135	0.1207	0.117	0.3731	0.1595	0.2515	0.01683	0.0143	2.5775

Mag. = Magnetite, Ilm. = Ilmenite, Leu. = Leucoxene, Ga. = Garnet, Rut. = Rutile,
Tit. = Titanite, Zr. = Zircon, Mz. = Monazite, Th. = Thorite, G. S.= Green Silicates,

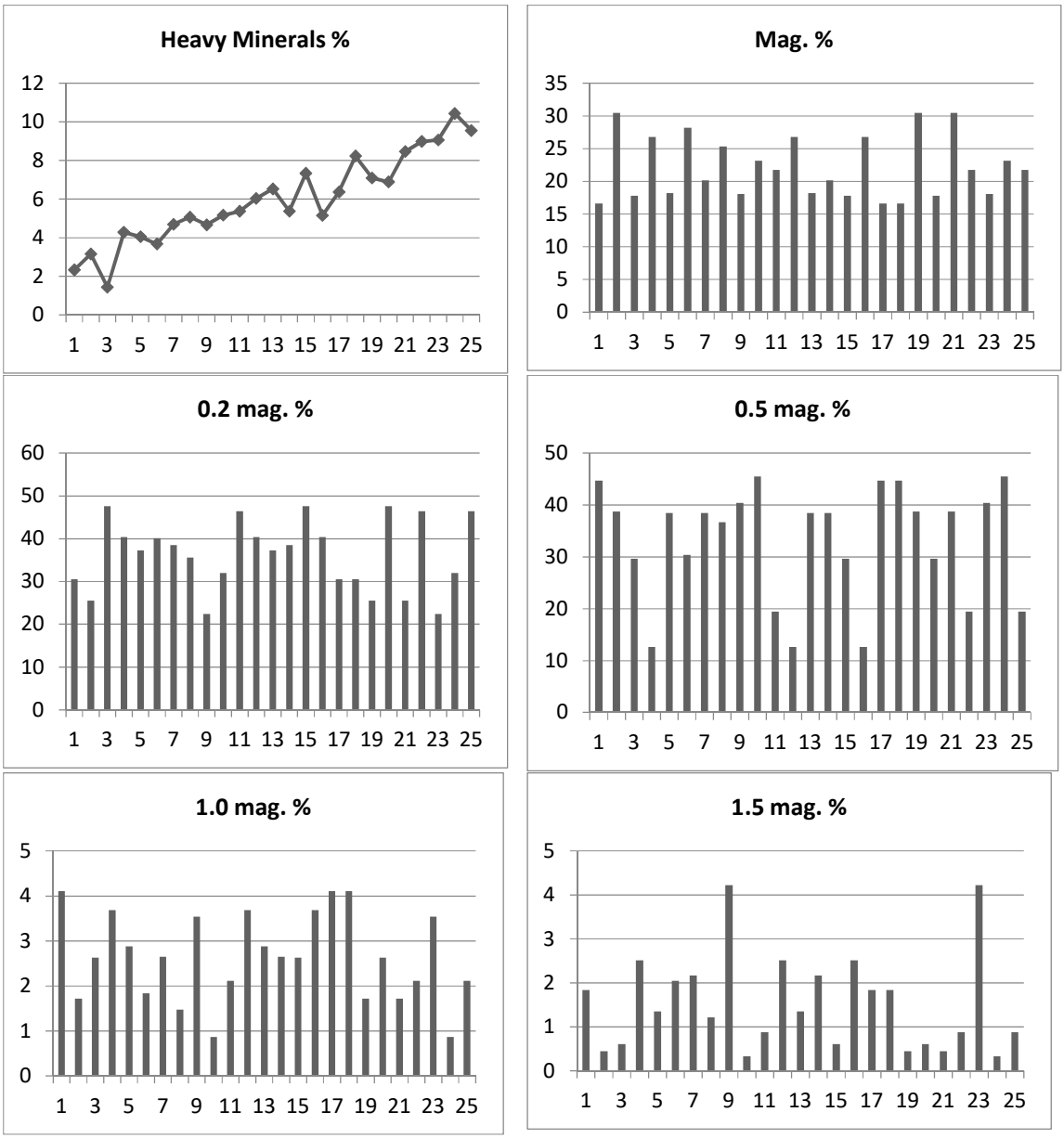

Fig. 3: Histograms of heavy minerals in the different magnetic fractions

Iron Oxides Minerals

Magnetite

It represents the major part of opaque grains of the studied samples. It is black granular masses (Fig. 4 a) and strongly magnetic, sometimes with zircon or garnet inclusions. It separated using small hand magnet. These mineral constituents range from 0.1% to 2.1 % with an average 1.097 % and represented by histogram (Fig. 4 b). The low uranium and thorium contents in magnetite of the stream sediments indicate that uranium in magnetite is mostly of the adsorbed type which is liable and easily leachable under the weathering conditions by meteoric water.

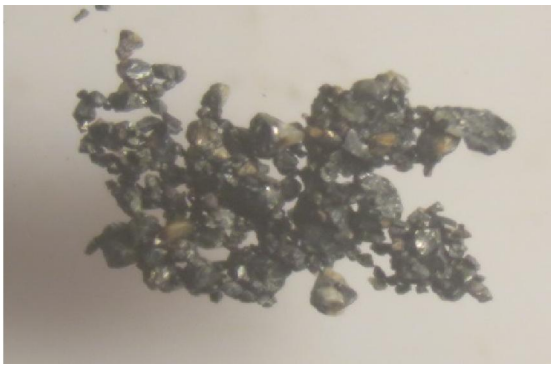

Fig. 4 a): Photo-micrograph of magnetite

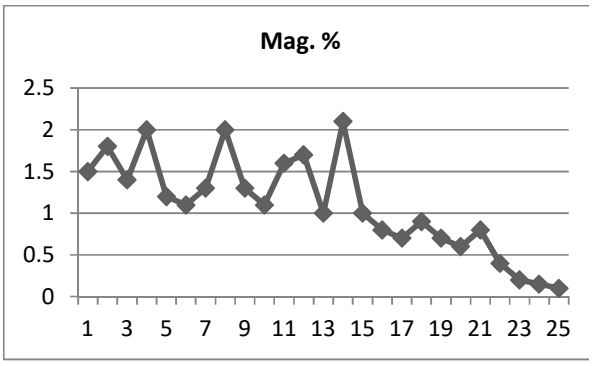

Fig. 4 b): Lateral distribution of magnetite

Ilmenite [Fe Ti O_3]

Ilmenite grains of the stream sediments may be altered. It concentrated in a relatively the highly magnetic fraction at 0.2 amp. It is the most abundant Fe-Ti oxide mineral that occurs in a wide variety of igneous rocks, some metamorphic rocks, and as detritus mineral grains. Ilmenite in the studied stream sediments occurs as irregular, tabular or massive to sub rounded angular grains (Fig. 5 a). These grains exhibit black to brownish black colors and submetallic to metallic luster. The brownish tint of some ilmenite grains may be due to the partial alteration of these grains. These mineral constituents range from 0.1 % to 0.9 % with an average of 0.3135 % and represented by histogram (Fig. 5 b).

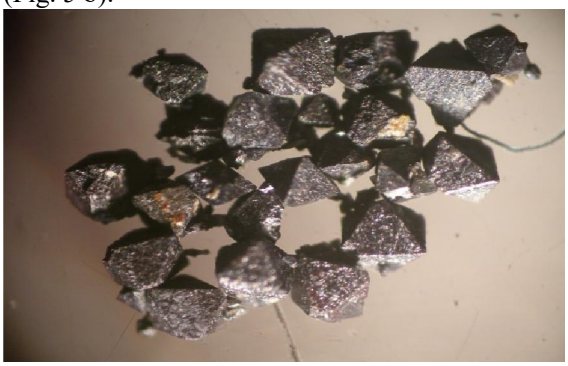

Fig. 5 a): Photo-micrograph of ilmenite

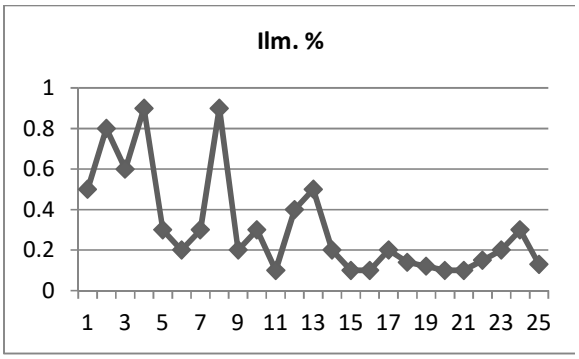

Fig. 5 b): Lateral distribution of ilmenite

Leucoxene

Leucoxene is an alteration product of ilmenite and is the transition stage between ilmenite and the secondary rutile. It is composed meanly from minute crystals of brookite and anatase. The leucoxene commonly occurs as rounded grains, opaque in transmitted light. A rough pitted surface is characteristic of most grains. The color of leucoxene grains varies from white, yellowish white to brown; it depends mainly on the degree of alteration, (Fig. 6 a). As the iron content decreases, the grain color becomes lighter brownish yellow, yellow, yellowish white and light creamy colors. Its specific gravity ranging from 0.01 to 0.4 with an average of 0.1207 % and represented by histogram (Fig. 5 b & c). According to the number of vugs formed in grains through iron withdrawal processes.

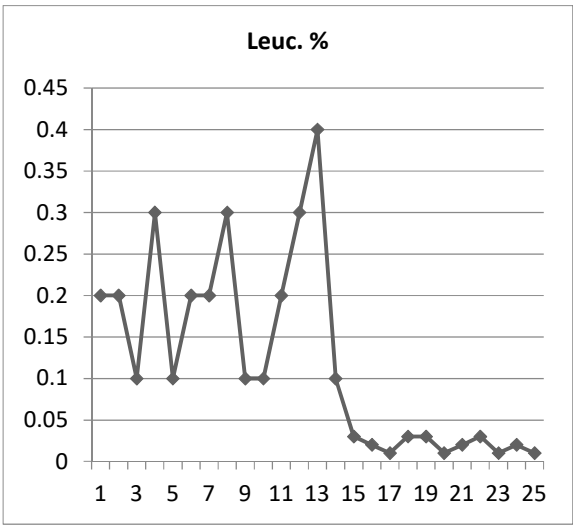

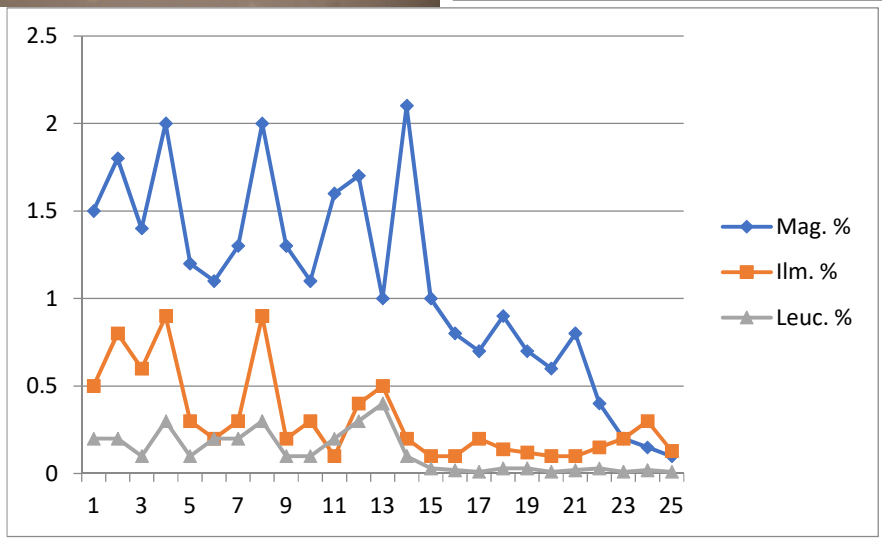

Fig. 6 a): Photo-micrograph of Leucoxene **Fig. 6 b):** Lateral distribution of Leucoxene
Fig. 6 c): Distribution of Opaque Minerals

Non Opaque Minerals

These minerals contain Garnet Group, Titanium minerals as Rutile, and Titanite (Sphene), Radioactive minerals as Zircon, Monazite and Thorite with Green Silicates. The description of these minerals illustrated in the following paragraph.

Garnet The minerals of garnet group characterize some metamorphic rocks and in some igneous rock types and can be noticed generally as detritus grains in sediments. It exhibits different colors ranging from pale pink to dark brown with vitreous luster. Sometimes garnet grains appear to be cloudy due to staining or inclusions (Fig. 7 a). The almandine type is the common garnet mineral in the studied samples probably due to the effect of contact or regional metamorphism. These mineral constituents range from 0.01 % to 0.4 % with an average of 0.117 % and represented by histogram (Fig. 7 b).

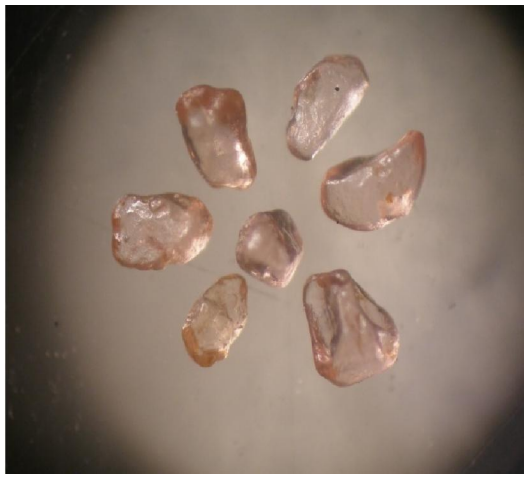

Fig. 7 a): Photo-micrograph of Garnet

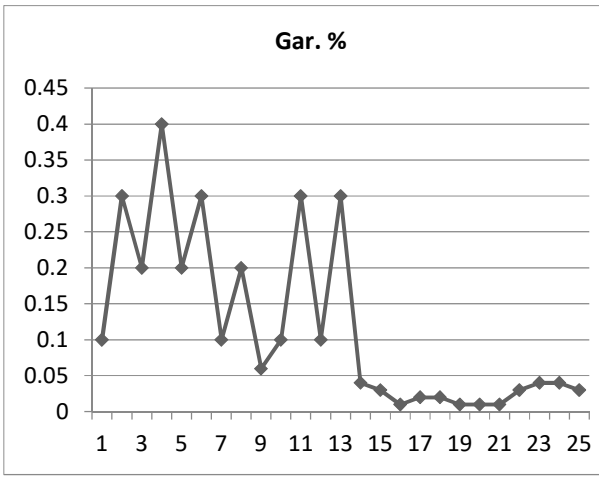

Fig. 7 b): Lateral distribution of Garnet

Titanium Minerals

Rutile [Ti O_2] It is the preferred mineral for the production of titanium dioxide. Rutile mineral grains are commonly prismatic, elongated, tabular and massive granular in shape. The common colors of rutile are reddish brown grading into the red (Fig. 8 a) and black with adamantine luster. These mineral constituents ranged from 0.1 % to 1.1 % with an average of 0.3731 %, and represented by histogram (Fig. 8 b).

Fig. 8 a): Photo-micrograph of Rutile

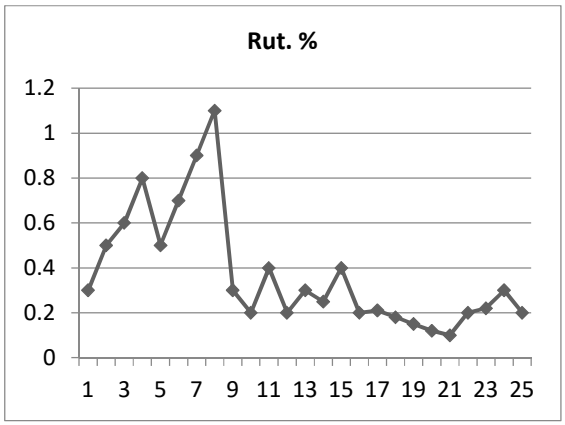

Fig. 8 b): Lateral distribution of Rutile

Titanite (Sphene) [Ca Ti Si O_5] It is widespread in acidic and intermediate igneous rocks and in several metamorphic rocks as accessory phase. It exhibits transparent to translucent yellow to yellowish brown colors (Fig. 9 a). Titanite mineral grains are subhedral to anhedral grains of adamantine luster and imperfect cleavage. The presence of titanite in the studied sediments was confirmed X-ray diffraction (Table 4). These mineral constituents ranged from 0.01% to 0.5% with an average of 0.1595% and represented by the histogram (Fig. 9b). Rutile and titanite show similarity of distribution and concentrate at upstream as in (Fig. 9c).

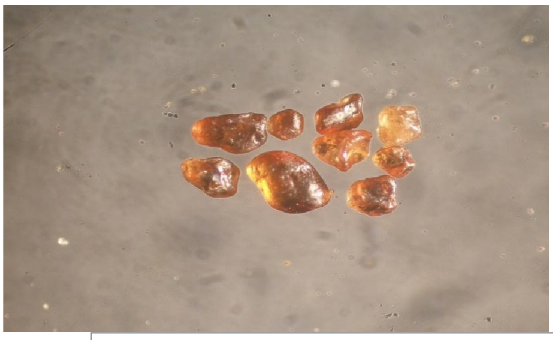

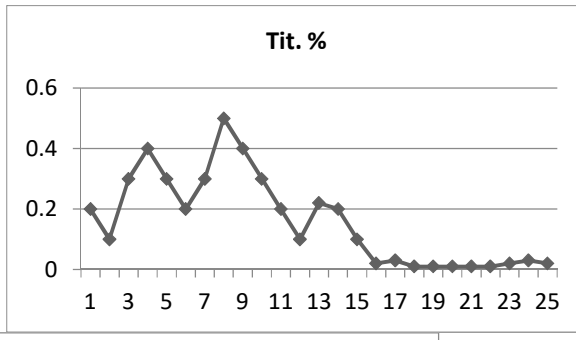

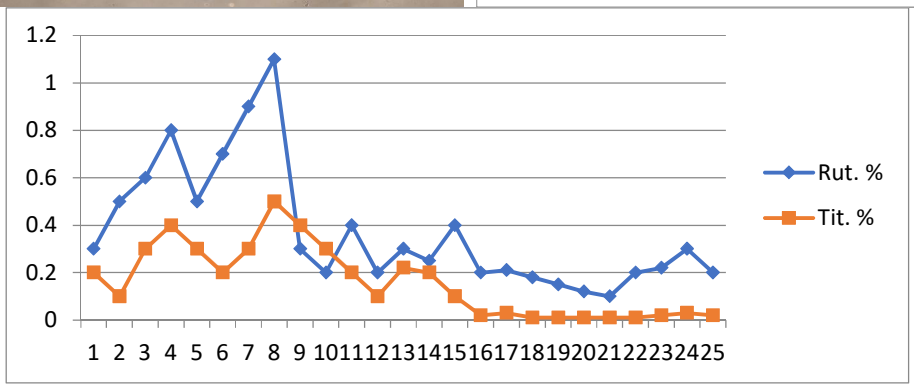

Fig. 9 a): Photo-micrograph of Sphene **Fig. 9 b):** Lateral distribution of Sphene
Fig. 9 c): Similarity of distribution and concentrate at upstream for Rutile and Titanite

Table 4: X-ray diffraction data of titanite of Wadi Abu Harba area.

Analysed Sample		Titanite ASTM card (11-446)	
dA	**I/I_o**	**dA**	**I/I_o**
7.22	6		
4.95	23	4.93	30
3.24	100	3.233	100
3.00	97	2.989	90
2.61	67		
2.59	55	2.595	90
2.29	19	2.273	30
2.07	27	2.058	40
1.65	24	1.643	40
1.50	17	1.494	4

Radioactive minerals

Zircon [Zr Si O_4] Zircon is a remarkable mineral due to its ubiquitous occurrence in crustal igneous, metamorphic and sedimentary rocks and in even mantle xenoliths, lunar rocks, meteorites and tektite (Speer, 1980). It occurs as an euhedral to subhedral grains, prismatic with bi-pyramidal termination (Fig. 10 a) and two bi-pyramidal. It is exhibiting brownish yellow colors of adamantine luster. These mineral constituents range from 0.02 % to 0.8 % with an average 0.2515 %, and represented by histogram (Fig. 10 b). (EDX) ESEM data indicate that zircon consists mainly of Zr O_2 and Si O_2 with trace amounts of Ca, Hf, Fe and Al (Fig. 10 c). The Zr / Hf ratio is a principle indicator of magmatic differentiation. The average Zr / Hf of zircon from granitoid rocks is 37.3, while this ratio reaches to 49.6 for volcanic rocks, 55.7 for basic rocks and 67 for ultrabasic rocks (Lyakhvich and Vishneveskiy, 1990). For the studied zircon, Zr / Hf ranges from 31.15 to 41.78, indicating that they derived from granitoid rocks. The presence of zircon in the studied sediments was confirmed X-ray diffraction (Table 5).

Table 5: X-ray diffraction data of zircon of Wadi Abu Harba area

Sample No.		Sample No.		Zircon ASTM Card No.6-266	
dA	I/I_0	dA	I/I_0	dA	I/I_0
10	45	4.434	32	4.48	4.43
100	100	3.302	100	3.35	3.30
3	8	2.650	5	2.64	2.65
20	45	2.518	38	2.54	2.52
5	10	2.336	6	2.35	2.35
29	8	2.217	5	2.24	2.07
10	20	2.066	16	2.08	1.75
---	12	1.751	8	1.76	---
---	40	1.712	24	1.72	---
---	14	1.651	10	1.66	---
---	8	1.477	5	1.48	---

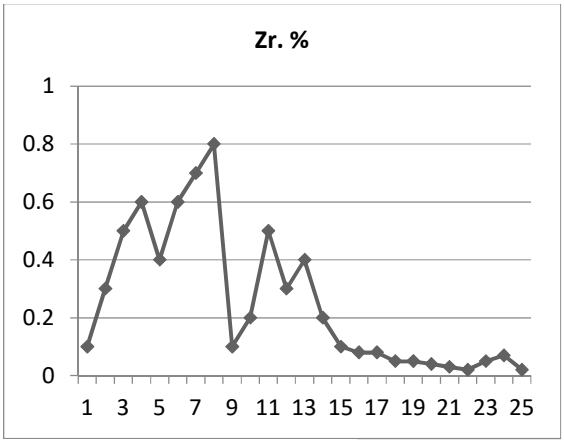

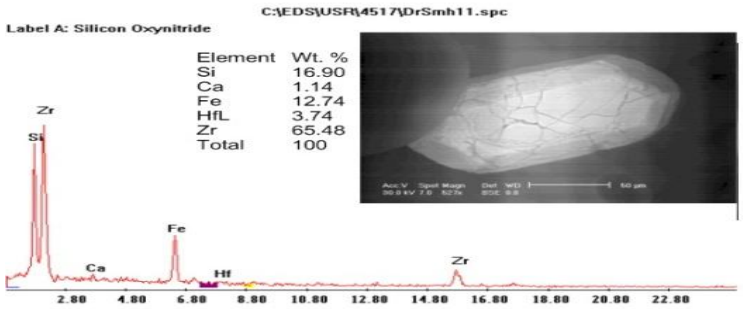

Fig. 10 a): Photo-micrograph for zircon **Fig. 10 b):** Histogram distribution of zircon
Fig. 10 c): ESEM zircon analysis

Monazite [Ce La PO_4]: It is one of the most important nuclear minerals, being a major host for REEs and actinides Th and U (Hinton and Paterson 1994, Bea *et al*. 1994, and Bea 1996). Monazite in the studied samples is rare in the heavy minerals of these samples. It forms tabular and broken crystals. Most of these grains are characterized by pitted surfaces. It is pale yellow, honey yellow, greenish yellow and reddish yellow color grains. These mineral constituents ranged from 0.001 % to 0.07 % with an average of 0.01683 % and represented by the histogram (Fig. 11 a & b). The EDX data (Fig. 11 c). The presence of monazite in the studied sediments was confirmed X-ray diffraction (Table 6).

Table 6: X-ray diffraction data of Monazite of Wadi Abu Harba area.

Sample No.		Monazite (11-556)	
d/A^0	**I/I_0**	**d/A^0**	**I/I_0**
4.19	13	4.17	25
3.51	38	3.51	25
3.31	50	3.30	50
3.10	100	3.09	100
2.87	35	2.87	70
2.15	19	2.15	25

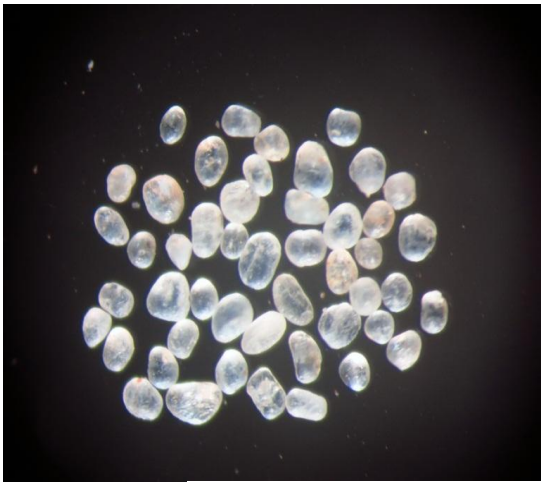

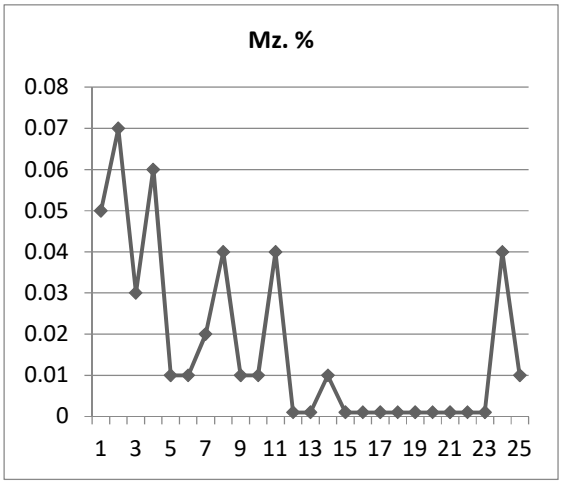

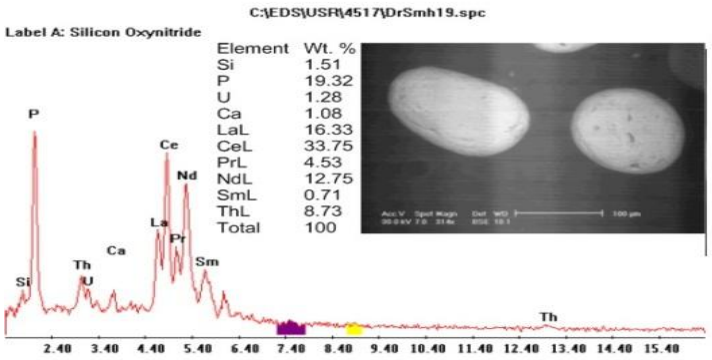

Fig. 11 a): Photo-micrograph of monazite **Fig. 11 b):** Histogram distribution of monazite
Fig. 11 c): (EDX) ESEM monazite

Thorite [Th Si O_4]: It occurs widely in the form of accessory minerals, which belong to the most important basic commercial minerals of thorium. It occurs as brownish black to black opaque grains of greasy luster (Fig. 12 a). Most of thorite mineral grains are subhedral to anhedral corroded and cracked. These mineral constituents range from 0.001 % to 0.03 % with an average 0.0143 %, and represented by histogram (Fig. 12 b). They are strongly metamictized, as determined by X-ray diffraction. In nature, thorite, generally, occurs in metamict state, amorphous to X-ray and electron diffraction, even though, they may have crystal faces (Ewing and Haaker 1980). Thorite was annealed at 1100˚C for approximately four hours preceding identification by XRD. The obtained data (Table 7) reveal the presence of thorite peaks (ASTM card 11-419) in addition to hematite peaks (ASTM card 13-534). The presence of hematite may be in the form of thin films coating thorite grains or as individual hematite grains. The ESEM analysis shows that thorite consists mainly of Th O_2 and Si O_2. Minor and trace elements include Y, U, Ca, Fe and REE.

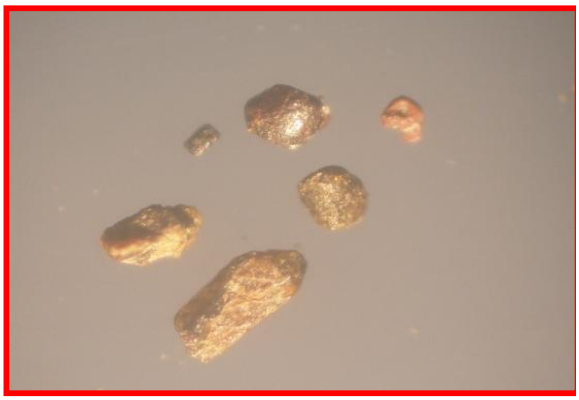

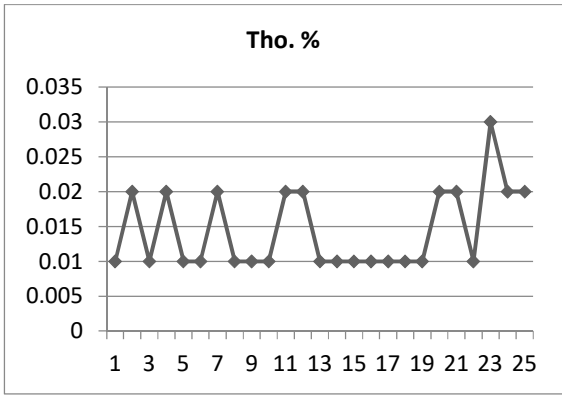

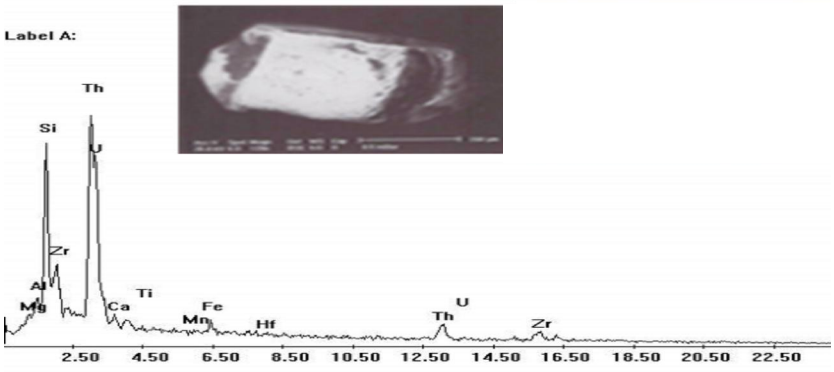

Fig. 12 a): Photo-micrograph of thorite **Fig. 12 b):** Histogram distribution of thorite
Fig. 12 c): (EDX) ESEM thorite

Table 7: X-ray diffraction data of Thorite of Wadi Abu Harba area

Analyzed Sample		Thorite ASTM card (11-419)		Hematite ASTM card (13-534)	
dA	**I/Io**	**dA**	**I/Io**	**dA**	**I/Io**
4.67	59	4.72	85		
3.54	100	3.55	100	3.66	25
2.82	21	2.842	45		
2.70	32			2.69	100
2.64	46	2.676	75		
2.52	21	2.516	30	2.51	50
2.34	3	2.361	5		
2.20	22	2.222	30	2.201	30
2.07	2			2.07	2
1.99	9	2.019	20		
1.87	15	1.885	30		
1.82	28	1.834	65	1.838	40
1.77	10	1.782	20		
1.69	12			1.69	60
1.65	8	1.667	10	1.634	4
1.48	5	1.484	20	1.484	35
1.43	4	1.444	15	1.453	35

Green Silicates (Amphiboles and Pyroxenes)

These minerals are consists of amphiboles, pyroxene, biotite, muscovite and epidote, and detected in the stream sediments. These minerals may have originated from igneous rocks. These minerals are characterized by coarse size detrital particles, black, green to pale green colour (Fig. 13 a) and has

medium to high magnetic success-ability. These mineral constituents range from 1.4 % to 3.78 % with an average of 2.5775 % and represented by histogram (Fig. 13b).

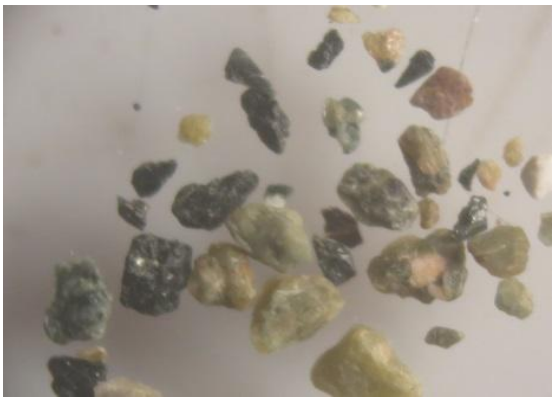

Fig. 13 a): Photo-micrograph of G. S.

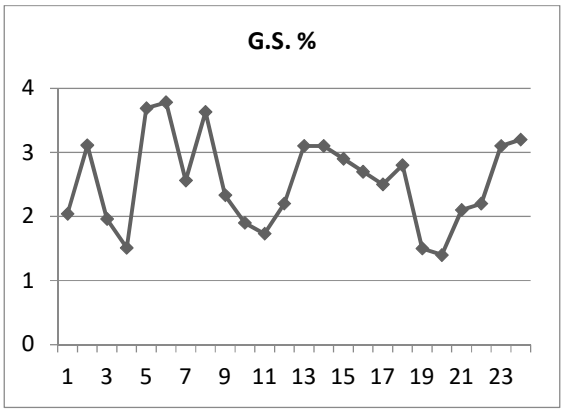

Fig. 13 b): Lateral distribution of G. S.

Geochemistry of trace elements

25 stream sediment samples were analyzed for the following trace elements: Cr, Ni, Cu, Zn, Zr, Rb, Y, Ba, Pb, Sr, Ga, V and Nb (Fig. 14). The results are shown in Table 8. From the obtained results, it can be concluded that these stream sediments are slightly enriched in Co, Rb, Ba, Sr and Nb (Compared with Upper Continental Crust (UCC), Rudinc and Gao., (2003) depleted in Ni, Cu, Zn and Y. High in Zr, Cr, Pb, V contents, which are higher than the UCC. The very high Ba content (995-1175 ppm), relative to other stream sediments of Egypt can be considered as a prominent geochemical signature of the study sediments. Thus, the abnormal enrichment of barium in the studied stream sediments point of view and in the hematized granitic rocks, 2195 ppm in average as well as in Hammamat sediments; 1135 ppm in average of W. Mayet El Abd area (El Balakssy, 2012) still a matter of contrivers and need more a detailed investigation. The enrichment of barium within the study area suppose that the area most probably affected by high intensive hydrothermal solutions. Besides, barium is normally considered to be captured by potassium-bearing phases during the differentiated sequence of the magma (Rankama and Sahama, 1950). Moreover, the highly differentiated granites are conventionally enriched in rare metals carriers such as zircon and monazite. Accordingly, it suggests that the mineralized granitic rocks dominating in the hinterlands of the study area are one of the main sources that provided the materials for enrichment. Meanwhile, Nb and Ba display weak negative relationships with the chemically analyzed U, whereas opposite trend with thorium has been encountered. This can be interpreted to the immobile nature of Th relative to U. Likely, Zr shows very weak positive correlation with both U and Th probably due to the low mobility of Zr, and implies that the studied zircon is partially significant carrier of U and Th. In addition, the elements; Zn, Rb, V and Ga are slightly enriched within the studied sediments. The present data on Zn and Rb are slightly higher than the average crustal values; 40 ppm. Rb correlates positively with the chemically analyzed U but negatively with Th. Vanadium may be genetically related to the anomalous concentration in the different rock types that encountered the studied area as the basic dykes; varies from 262 to 304 ppm, Hammamat sediments; 121 ppm and the altered granites varies from 136 to 141 ppm as perceived earlier by El Balakssy (2012). On the other hand, some base metals as Cr, Ni and Cu are depleted in the concerned sediments; presumably due to the absence of the basic rocks in the studied area. In addition, a remarkable depletion in Pb was noticed; it is below detection limit, their deficiency may be attributed to the lack of lead-bearing minerals. The sediments was also found to contain relative low Sr content; varies from 15 to 36 ppm, it lie within the typical range of the average crustal values; 20 ppm. Since strontium is considered as a mobile element in both oxidizing and reducing conditions, it is possible that the strontium was leached out of the granitic

rocks and redeposited in stream sediments or minor addition from the basic dykes; 411 to 531 ppm as well as the Hammamat sediments; 41 to 50 ppm (El Balakssy, 2012).

Furthermore, the studied stream sedimentary samples commonly show slightly low REE contents compared with the granitic rocks of the studied area. It ranges from 65 to 223 ppm, whereas the granitic rocks show REE contents ranging between 276 and 344 ppm (El Balakssy, 2012). The depletion of REE in these sediments is probably results from the mobilization process by groundwater circulation, dilution of REE by mixing with sediments and/or reworked weathered granitic rocks. The result is confirmed by markedly good correlation with the chemically measured U but not with Th. Another results showed that the deeper sedimentary samples are relatively enriched with REE; up to 223 ppm than surface samples; up to 65 ppm which may have also been reflected the mobility of some REE towards the subsurface portion and indicating potential for mineralization. Consequently, the remarkable depletion or addition in certain element indicates the disturbance in the dynamic equilibrium of the elemental concentrations system, leading to local changes in the stream ecosystem balance, where some elements are greatly increased on the expense of others. The enrichment or depletion in certain elements reflects the geology, geochemistry and mineralogy of the source regions and considered a function of a complex series of interactions between hydrothermal fluids, host rocks, groundwater and surface waters.

Table 8: Trace Elements Concentrations in Wadi Abu Harba stream sediments

S. No.	Cr	Co	Ni	Cu	Zn	Zr	Rb	Y	Ba	Pb	Sr	V	Nb
1	89	15	47	29	68	20	80	23	600	20	310	111	11
2	91	17	49	28	67	21	74	25	597	22	318	103	10
3	90	14	55	27	66	19	72	22	598	21	295	106	9
4	93	16	49	26	65	19	85	18	633	15	309	101	12
5	100	16	46	30	70	20	82	20	640	18	300	102	9
6	97	15	60	28	63	18	84	19	637	16	305	100	12
7	99	15	49	31	71	22	80	22	611	20	299	99	9
8	95	17	47	28	64	21	77	17	630	16	289	89	10
9	98	16	54	29	67	20	79	19	625	17	294	95	8
10	101	15	47	28	63	19	79	19	587	14	314	100	9
11	92	17	49	30	67	18	84	21	641	20	318	98	12
12	100	14	46	28	65	17	82	20	594	17	315	99	10
13	87	15	45	29	69	23	82	20	599	21	316	96	11
14	89	17	50	30	70	21	80	23	636	19	307	104	10
15	86	14	43	27	68	20	81	21	615	18	312	100	9
16	103	16	48	29	65	20	78	22	642	16	311	109	9
17	90	15	48	28	68	21	75	18	609	14	309	104	11
18	95	16	46	27	66	19	76	19	634	17	306	105	8
19	89	17	46	30	68	19	80	20	622	20	317	100	10
20	90	15	45	28	70	21	79	22	626	19	318	99	11
21	97	16	49	30	64	22	83	19	609	22	308	95	10
22	90	17	44	27	67	20	81	20	620	18	312	97	9
23	93	15	45	28	66	21	80	17	610	19	306	98	8
24	88	16	41	25	63	19	78	18	598	17	301	95	10
25	89	14	48	27	70	23	73	20	610	21	304	90	11
Min.	86	14	41	25	63	17	72	17	587	14	289	89	8
Max.	103	17	60	31	71	23	85	25	642	22	318	111	12
Av.	93.24	15.6	47.84	28.28	66.8	20.12	79.36	20.16	616.92	18.28	307.72	99.8	9.92
UCC	100	17.5	47	28	67	19.3	84	21	628	17	320	97	12

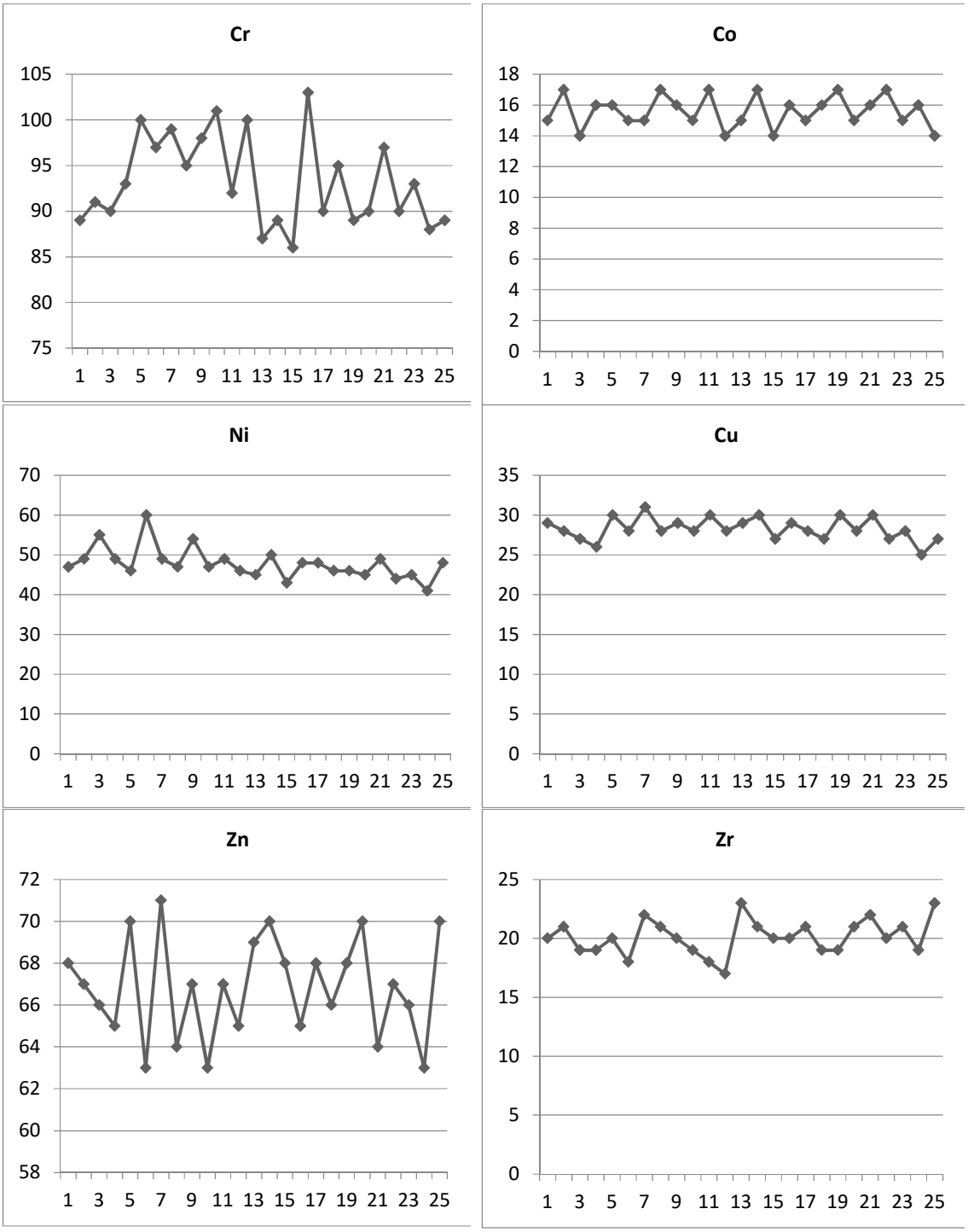

Fig. 14 a): Lateral distribution of Cr
Fig. 14 b): Lateral distribution of Co
Fig. 14 c): Lateral distribution of Ni
Fig. 14 d): Lateral distribution of Cu
Fig. 14 e): Lateral distribution of Zn
Fig. 14 f): Lateral distribution of Zr

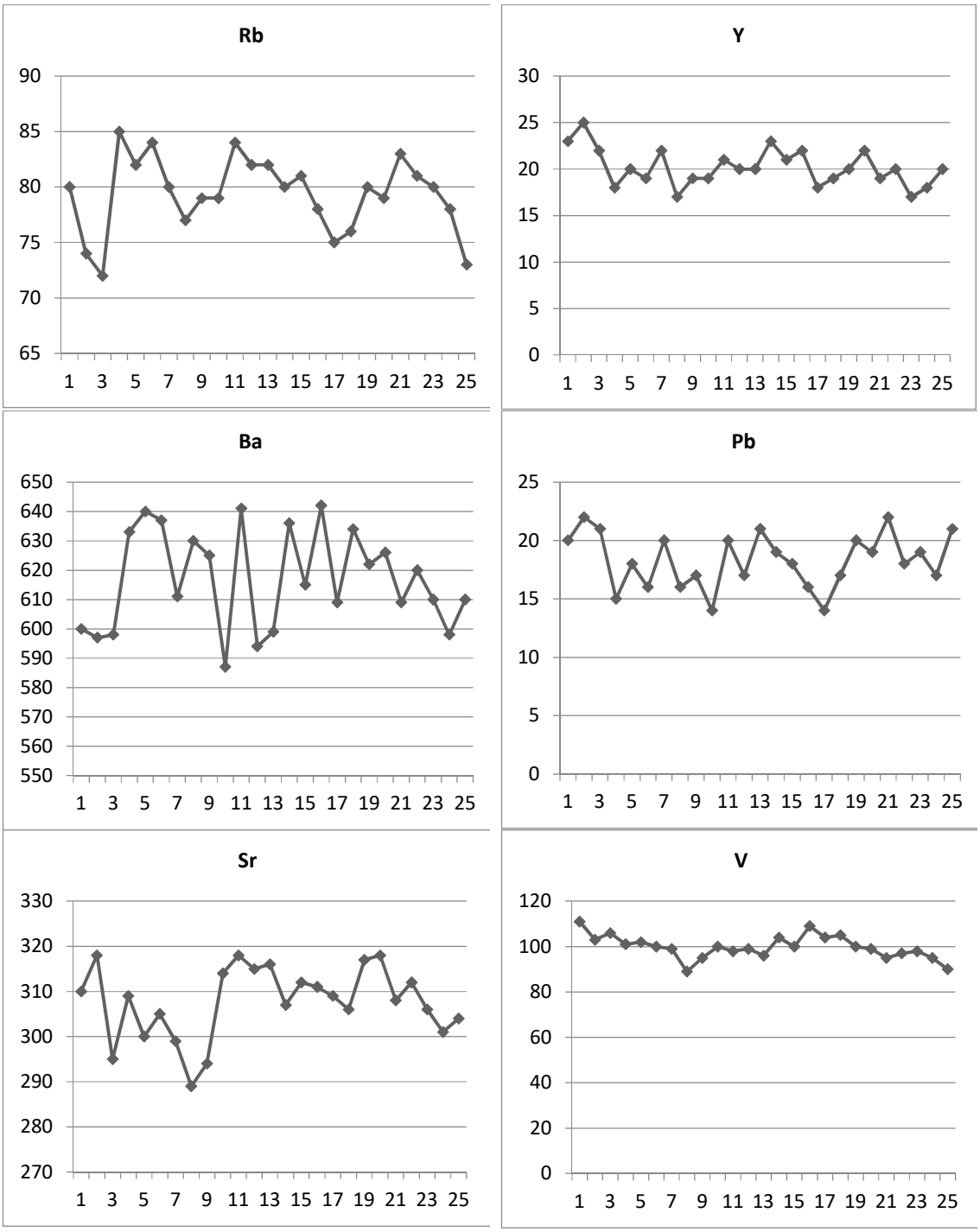

Fig. 14 g): Lateral distribution of Rb
Fig. 14 h): Lateral distribution of Y
Fig. 14 i): Lateral distribution of Ba
Fig. 14 j): Lateral distribution of Pb
Fig. 14 k): Lateral distribution of Sr
Fig. 14 l): Lateral distribution of V

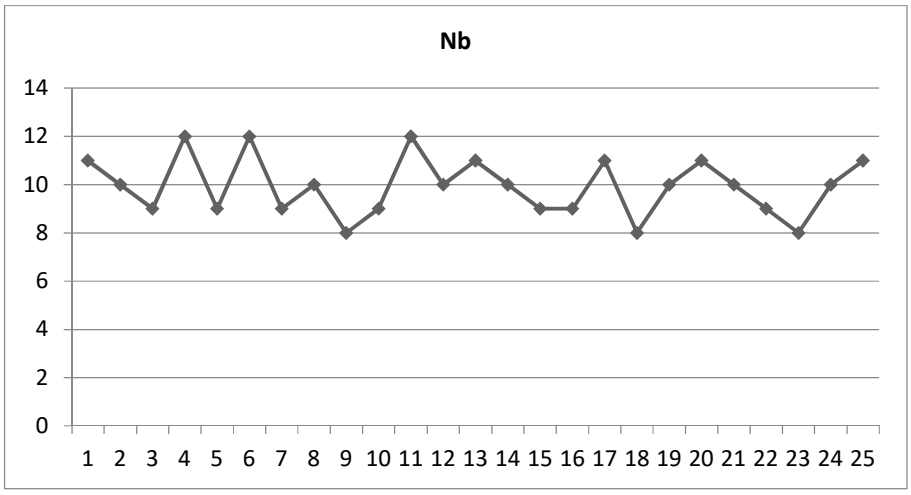

Fig. 14 m : Lateral distribution of Nb

Radioactivity

Radiometrically measured uranium and thorium contents reveal that the studied stream sediments are much enriched in thorium over uranium (Table 9). The average content of chemically-U is as much as 15 ppm, while Th exceeds 65 ppm may be due to the relative enrichment of thorium-bearing minerals. Meanwhile, the fresh younger grants of the study area have average content of chemically-U and Th as 25 ppm and 45 ppm respectively (El Balakssy, 2012). Additionally, the calculated eU/U and eTh/U ratios (Table 3) are mostly more than unity revealing that a selective leaching of uranium content compared with the stable thorium during the supergene processes; under favorable pH conditions. The obtained results coincide with the fact that reached by Hansink (1976), where the greater eU/U and eTh/U ratios indicate recent U loss. Also, the reverse relationships between the chemically measured U and Th as well as U and Th/U ratio may corroborate the mobilization of uranium which can be precipitated in the sediments through the pore fluids as authigenic uranium. According to Jones and Manning (1994) the authigenic uranium can be calculated from data gathered by the chemical measurements and shown in the formula:

$$[Ua] = [U]-[Th/3]$$

Where: Ua is the authigenic uranium U is the total present U & Th/3 is equivalent to original U where this three times as abundant in igneous rocks (Rogers and Adams, 1969). Generally, the authigenic U was formed in situ within the depositional site in response to geochemical processes. Their precipitation in sediments indicating chemically reducing conditions but under oxidizing ones leads to remobilization of authigenic U. In the present study, such uranium displays negative values that confirm the mobilization of uranium relative to thorium. The leaching leading to disequilibrium is markedly obvious in shallower samples. Remarkably, the highly mobile U6+ could infiltrate downward and trapped by the impermeable silt-size fractions. Here, some of the liberated uranium is mostly reprecipitated as complexes uranium species depending on the anions in the hydrothermal solutions (Abdel Monem *et al*., 1998). Consequently, these sediments appear to be as a slightly favorable delivery pools for thorium rather than uranium which is probably due to either the relative abundance of the thorium- bearing minerals or the selective leaching processes of uranium throughout supergene processes. Ra probably remains in the sediments with no significant loss.

Distribution of U and Th

The examined stream sediments of Wadi Abu Harba are characterized by radiometrically low concentrations of U and Th. The radiometrically elemental concentration of U range between 1 and 4ppm with an average 2.9ppm, while it is between 8 and 28ppm for Th with an average 17ppm. The average Ra content for these sediments is 2.8ppm, ranging between 1 and 4ppm.

eU versus eTh variation diagram

The relation between U and Th may indicate the enrichment or depletion of U because Th is chemically stable. The eU against eTh variation diagram for the studied samples is shown in (Fig. 15a), which indicates strong positive relationships between the two elements. This result explains the

low alteration processes affecting these samples, and also indicates that magmatic processes played an important role in the uranium enrichment of these granites which represent the source of these sediments.

eU versus Zr variation diagram

The eU versus Zr variation diagram shows strong positive correlation in the studied samples (Fig. 15b). The uranium and zirconium enrichment in the studied samples, supports the concept that U was trapped in the accessory minerals as zircon and the uranium is magmatically.

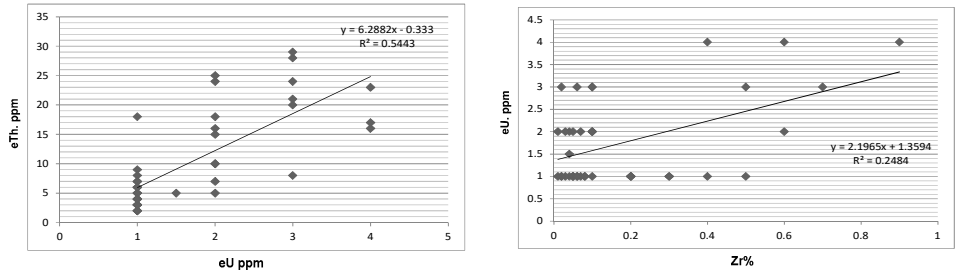

Fig. 15a): Direct relationship between equivalent uranium and equivalent thorium.
Fig. 15b): Direct relationship between eU and concentration of Zr minerals. r= 0.7 r= 0.5

Table 9: eU, eTh, Ra (ppm) and K (%) content of the Abu Hamur stream sediments

S. No	eU (ppm)	eTh (ppm)	Ra (ppm)	K (%)	eTh/eU	ARs (eU/Ra)
S1	2	10	1	1.48	5	2
S2	1	18	2	1.56	18	0.5
S3	3	20	3	1.12	6.7	1
S4	4	16	2	1.05	4	2
S5	4	17	3	1.07	4.25	1.33
S6	2	24	4	1.01	12	0.5
S7	3	28	4	1.18	9.33	0.75
S8	4	23	4	0.92	5.75	1
S9	2	10	3	1.04	5	0.66
S10	1	9	3	1.27	9	0.33
S11	1	8	2	0.92	8	0.5
S12	1	7	1	1.48	7	1
S13	1	6	2	1.56	6	0.5
S14	1	7	3	1.12	7	0.33
S15	1	5	2	1.05	5	0.5
S16	1	4	3	1.07	4	0.33
S17	1	6	4	1.01	6	0.25
S18	1	3	4	1.18	3	0.25
S19	1	5	4	0.92	5	0.25
S20	1	4	3	1.04	4	0.33
S21	1	3	3	1.27	3	0.33
S22	1	2	2	0.92	2	0.5
S23	1	2	2	0.10	2	0.5
S24	1	2	1	1.48	2	1
S25	1	2	2	1.56	2	0.5
Min.	1	2	1	0.10	2	0.25
Max.	4	28	4	1.56	18	1.33
Ave.	1.64	9.64	2.6	1.14	5.40	0.38

Conclusion

The study concerned with the study of economic minerals in the stream sediments of Wadi Abu Harba which has long 200 km. The area covered by igneous and metamorphic rocks and younger granite.

The area affected by different faults and represented by strike-slip faults. The normal faults are only preserved on a minor scale along these strike-slip faults represented by nearly vertical slickensides that indicate to substantial vertical displacement.

The average content of total heavy minerals is 5.96 % and the heavy content ranging from 1.45 % and 10.45 %. The heavy minerals represented by 1.098 % magnetite, 0.3136 % ilmenite, 0.1208 % leucoxene, 0.3732 % rutile, 0.2516 % zircon, 0.01684 % monazite, 0.118 % garnet and 0.1596 % titanite. Radiometric analysis revealed that the average equivalent uranium content (eU) is 1.64 ppm and the average equivalent thorium is (eTh) is 9.64 ppm.

The concentration of minerals restricted in the downstream and upstream, the parts of the area due to the present of acidic rocks and the geomorphology of wadis.

The transportation agent is rare and consider seasonal so the sediment restricted near the source rock and transported short distance.

References

Abd El Atty, 2013. Mineralogical and geochemical studies of the uranium – bearing granites, Gabal Abu Harba area, North Eastern Desert, Egypt, Ph. D. Thesis, Faculty of Science, Benha University.

Abdel Monem *et al*., 1998. Effect of different dietary levels of inorganic zinc oxide on ovarian activates, reproductive performance of Egyptian Baladiewes and growth of there lambs, Vol. 14. No. 2, 116 – 123 ref. 30

Akaad, M. K., S. El-Gaby and M. E. Habib, 1973. The Barud Gneisses and the origin of Grey Granite. Bull. Fac. Sci. Assiut Univ. 2, 55–69.

Bea, F., 1996. Residence of REE, Y, Th and U in granites and crustal protolith; implications for the chemistry of crustal melt. J. Petrol., Vol. 37, P. 521:552.

Bea, F., M. D. Pereira, L. G. Corretage and G. B. Fershtater, 1994. Differentiation of strongly peraluminous, perphosphorous granites: the Pedrobenards pluton, Central Spain. Geochemica et Cosmochemica Acta, Vol. 58, P. 2609:2627.

El Balakssy, 2012. Mineralogical, geochemical and radioactive aspects of Nuweibi basement rocks, Central Eastern Desert, Egypt. Volume 34, Issue 1, Pages 10 – 34.

Ewing, R. C. and R. F. Haaker, 1980. The metamict state: Implications for radiation damage in crystalline waste forms. Nuclear and Chemical Waste Management, I, P. 51:57.

Folk, R.L., 1980. Petrology of sedimentary rocks. Univ. Texas, Hemphill, Pup. Co. Austin, Texas, USA.

Hansink, J.D., 1976. Equilibrium analysis of a sandstone rollfront uranium deposit, Proceeding Intr. Symposium on exploration of uranium ore deposits, AEA, Vienna, p: 683-693.

Hinton, R. W. and B. A. Paterson, 1994. Crystallization history of granitic magma: evidences from trace elements zoning. Mineral. Mag., Vol. 58A, P. 416:417.

Jones and Manning, 1994. Comparison of Geochemical Indices Used of Interpretation of Palaeoredox Conditions in Ancient Mudstones. Chemical Geology, 111. 111-129.

Lyakhvich, V. V. and A. A. Vishnevskiy, 1990. Zr and Hf in rapakivi zircons and the origin of avoids. Geokhimiya. Vol. 8, P. 1075:1083.

Rankama and Sahama, 1950. International Journal of Geosciences, Vol. 6 No. 4.

Rogers, J.J.W. and J.S.S. Adams, 1969. Uranium. In : Wedepohl, K. H. (ed.) Handbook of geochemistry, New York, Springer - Verlag, 4: 92 B1 to 92 C10.

Rudinc & Gao., 2003. Government Auditing Standards and revision 162.

Sabet, A.H., S. El-Gaby and A.A. Zalata, 1972. Geology of the basement rocks in the northern parts of El-Shayib and Safaga Sheets, Eastern Desert. Ann. Geol. Surv. Egypt II, 111–128.

Speer, J. A., 1980. Zircon. In P.H. Ribble [2nd ed.]. Reviews in Mineralogy 5: Orthosilicate Mineral Soc. Am., Washington D. C., P. 67:112.